



Hybrid ResNet50-SVM Framework for Detecting Brain Tumors from MRI Images

Zouhir Iourzikene¹, FawziGougam², Djamel Benazzouz³

Laboratoire Mécanique des Solides et Systèmes (LMSS), Faculté de Technologie, Université M'Hamed BOUGARA de Boumerdes, 35000 Boumerdes, Algeria

*Corresponding author.z.iourzikene@univ-boumerdes.dz; f.gougam@univ-boumerdes.dz; d.benazzouz@univ-boumerdes.dz

Received. June 17, 2024. Accepted. December 06, 2024. Published. December 20, 2024.

DOI: <https://doi.org/10.58681/ajrt.25090104>

Abstract. Brain tumors are abnormal cell proliferations that may develop within the brain and can be either non-cancerous (benign) or cancerous (malignant). They might arise primarily in the brain or spread to it from other regions through metastasis. The task of classifying brain images obtained from Magnetic Resonance Imaging (MRI) has gained significant importance in medical research. Recent studies increasingly adopt machine learning approaches to build predictive and diagnostic tools for healthcare applications. This study proposes a method for brain tumor detection using various MRI brain scans. Features are extracted by employing the ResNet50 deep convolutional neural network architecture. Subsequently, classification models based on Support Vector Machines (SVM) are implemented to perform tumor prediction.

Keywords. Cancer brain, MRI, Extraction features, SVM, Deep learning.

INTRODUCTION

Brain tumors encompass a diverse and complex group of tumors affecting the central nervous system. According to the World Health Organization (WHO), nearly a hundred distinct types have been identified, primarily classified through pathological evaluation (Lesniak, 2004). These tumors are generally categorized as either benign or malignant, with the WHO introducing a grading scale ranging from I to IV. Tumors assigned to grades I and II are typically regarded as low-grade or non-cancerous, whereas those classified as grades III and IV are considered high-grade or malignant (Barnholtz-Sloan, 2018).

To evaluate the characteristics of these tumors, several diagnostic tools are employed. Among them, Magnetic Resonance Imaging (MRI) and Computed Tomography (CT) are

currently regarded as the most effective techniques for distinguishing between healthy and abnormal brain tissues. CT scans utilize X-rays and advanced computer processing to generate detailed cross-sectional images of the brain for clinical assessment (Alsubai, 2022).

Image processing techniques (contrast, segmentation, filtering, mathematical morphology ...) allow the extraction of important information and characteristics (contours, edge detection, object detection ...). This information can guide and monitor interventions after the detection and localization of the disease, to plan and treat the disease efficiently (Gordillo, 2013).

Early detection of malignant tumors (clusters of cancer cells) plays an essential role in cancer diagnosis, to precancerous lesions at a more curable stage, and facilitate diagnosis before the disease is at an advanced stage, which allows for lighter and more effective treatment, and may improve long-term survival. For this purpose, Machine Learning (ML) methods are designed to build computational models capable of analyzing input data and generating predictions through statistical inference. These techniques enable systems to automatically learn from data patterns without requiring manually coded instructions (Fernandez, 2019).

In recent years, concerns about the limitations in prediction precision and the sensitivity of medical data have led researchers to explore more advanced solutions for brain tumor detection. Deep Learning (DL), a specialized branch within ML, has emerged as a promising approach due to its capacity to develop highly accurate and efficient predictive models (Noreen, 2020). DL algorithms use many layers, linked together by connectors (synapses). From there, it processes information through a propagation model of these cellular activations, activations above a certain threshold (Sultan, 2019). Deep learning is used in multiple settings, including image recognition, language processing, robotics, speech recognition, and bioinformatics.

The classification of images by machine learning, neural networks, and deep learning, essentially needs a bag of features of our images, to make it a better classification and more than the selection of deep features more than we get better accuracy. In recent years deep learning is used a lot because it gives accuracy results. In this study, two approaches have been proposed to assist healthcare professionals, including radiologists and surgeons, in the diagnosis of brain tumors using MRI scans. The first method consists of selecting and classifying images according to healthy or tumor MRI using ResNet50. Our database contains a set of images where some of them are without tumor and other with tumor. The approach developed uses 70% training and 30% testing. Results in identifying images containing tumors are 89%. Due to this percentage of the first method we thought that it is necessary to be more accurate in the identification. Thus, the second approach is a hybrid method combining ResNet50 and Support Vector Machine. The reason of this combination is motivated by the fact to take advantages from the convolution neuron network which gives a bag of features more important than other methods, second the SVM gives better results of classification. Different SVM classification methods are used to detect and classify our MRI images from feature bags obtained by ResNet50. We obtain the same accuracy rate of 92% by using the Linear SVM and Quadratic SVM. By the Cubic SVM we obtain an accuracy rate of 93%, and finally by the Medium Gaussian SVM we obtain the best classification by an accuracy rate of 94% (Chinnam, 2019; Blumenthal, 2017). All these methods are learned by the bag of features of matrix form of size (546 1000), such that the rows of this matrix represent the number of images trained by ResNet50, the columns are the number of features of MRI images selected by ResNet50, the training and testing of these classification methods are split 70% training and 30% test.

Before classifying our MRI images, the selection of features was performed using a convolutional neural network (CNN) ResNet50 model to obtain bag of features in the form of a matrix. This was used in SVM to improve the performance classification accuracy. First, we preprocess our MRI images, adjustment is used to enhance histogram contrast and filled them

to improve edge filtering. Then, the Otsu segmentation is applied to choose an automatic threshold from the histogram, which is separated into two classes, black and white for each image. Finally, the mathematical morphology is the erosion followed by the dilation by structuring element gamma four. The process of pixel subtraction was employed to delineate object contours in MRI images, including both their outer perimeters and the internal separations corresponding to holes in the binary format (Abbood, 2021; Anitha, 2016).

RELATED WORKS

Recent studies have increasingly focused on applying AI techniques, especially DL and ML methods, to improve the accuracy of brain tumor identification and categorization using MRI scans.

Biswas et al. (2023) proposed an integrated approach that leverages both CNN and SVM to enhance the accuracy of brain tumor classification. Their method included several preprocessing operations such as resizing the input images, reducing noise using an edge-preserving anisotropic filtering technique, and improving image contrast through the application of adaptive histogram-based equalization, along with data augmentation to increase variability. The deep CNN automatically extracted meaningful features, which were then classified using SVM. When tested on the Figshare dataset, the proposed approach reached an accuracy of 96%, outperforming well-known transfer learning architectures such as AlexNet, GoogLeNet, and VGG16, with the added advantage of lower computational demands.

Suryawanshi et al. (2024) introduced a combined framework that integrates convolutional neural networks (CNNs) with the pre-trained VGG19 architecture for feature extraction, followed by a support vector machine (SVM) classifier to handle multiclass brain tumor identification. The approach, evaluated on the BRATS and Sartaj datasets, achieved notable accuracy in differentiating tumor categories, emphasizing the benefits of blending deep learning with SVM-based classification in medical imaging.

Basthikodi et al (2024) developed a multiclass brain tumor classification method by combining SVM with feature extraction techniques (HOG, LBP) and dimensionality reduction using PCA. Using a Kaggle dataset with four tumor types, their model achieved an accuracy of 96.03%. The integration of HOG, LBP, and PCA enhanced classification performance and reduced overfitting, making the approach more efficient and robust.

Özkaraca et al. (2023) proposed a novel deep learning framework that integrates various pretrained architectures—including DenseNet, VGG16, and standard CNNs—leveraging their advantages while addressing known weaknesses in brain tumor classification. The proposed model attained an accuracy of 98.5%, though it exhibited a relatively high computational cost. To assess the model's performance, the authors applied a validation protocol combining an 80/20 training-to-testing ratio with 10-fold cross-validation.

SAMAR M. ALQHTANI (2024) introduced a fully automated approach for segmenting and classifying brain tumors from MRI scans. The process included a preprocessing phase involving Contrast Limited Adaptive Histogram Equalization (CLAHE) and diffusion-based noise filtering. Tumor regions were segmented using the Fuzzy C-Means (FCM) clustering algorithm, and the classification stage employed a Support Vector Machine (SVM). The method, validated on the CE-MRI dataset, reached a classification accuracy of 98.2%, with a sensitivity of 97.7%, specificity of 97.9%, and a Dice similarity coefficient of 96.1%. Furthermore, it demonstrated rapid execution, requiring only 0.42 seconds per image, outperforming prior methods in terms of both precision and processing speed.

In her study, SoheilaSaeedi(2023) focused on the early detection of brain tumors by employing both deep learning and traditional machine learning techniques. A dataset comprising 3,264 MRI scans was utilized to differentiate between gliomas, meningiomas,

pituitary adenomas, and non-tumorous (healthy) brain images. The research introduced a two-dimensional convolutional neural network (2D CNN) alongside a convolutional autoencoder model. The CNN achieved an accuracy rate of 96.47%, while the autoencoder reached 95.63%. Additionally, six machine learning algorithms were evaluated, among which the K-Nearest Neighbors (KNN) method obtained the best performance with 86% accuracy. Overall, the 2D CNN model demonstrated superior classification capabilities compared to the others, with an area under the ROC curve approaching 1, highlighting its robustness and clinical potential in tumor identification.

This research underscores the strong potential of artificial intelligence methods in facilitating timely diagnosis and accurate categorization of brain neoplasms, through the use of diverse models demonstrating notable precision and computational effectiveness.

SVM AND CNN OVERVIEW

SVM are supervised learning techniques widely applied to both classification and regression tasks (Fan, 2005). They have been effectively utilized in various domains, including medical signal analysis, natural language processing, speech recognition, and image analysis (Cristianini, 2000).

In classification contexts, SVMs aim to identify an optimal hyperplane that separates data points from different classes. Ideally, this hyperplane maximizes the margin—the largest possible distance between the two classes—illustrated by the boundaries marked with plus and minus signs in Fig. 1. The margin refers to the widest zone around the hyperplane that remains free of data points. While such a clear separation is possible for linearly separable datasets, real-world scenarios often involve overlapping classes. To address this, SVMs employ a soft margin strategy, which permits limited misclassifications to enhance the model's generalization capability (Ruppert, 2004).

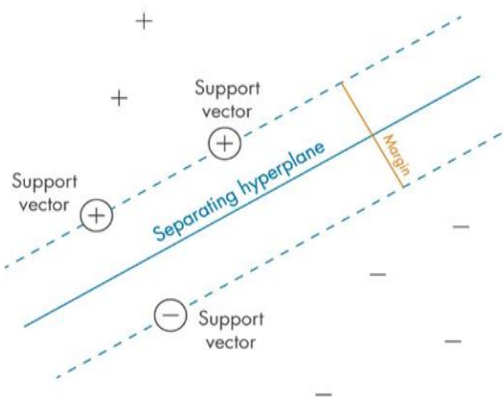


Fig. 1. Establishing the margin that separates different classes is the core objective optimized by the SVM algorithm.

Deep learning architectures are particularly effective when trained on large-scale datasets, while conventional machine learning algorithms often reach a performance plateau beyond a certain data threshold.

Convolutional Neural Networks (CNNs) represent a deep learning framework capable of learning relevant features directly from raw input data, eliminating the need for manual feature engineering (Fig. 2) (Ren, 2015). These networks are especially powerful in identifying complex visual patterns, enabling applications such as object, face, and scene recognition. Moreover, CNNs have demonstrated strong performance in classification tasks involving non-image data as well (Zitnick, 2014).

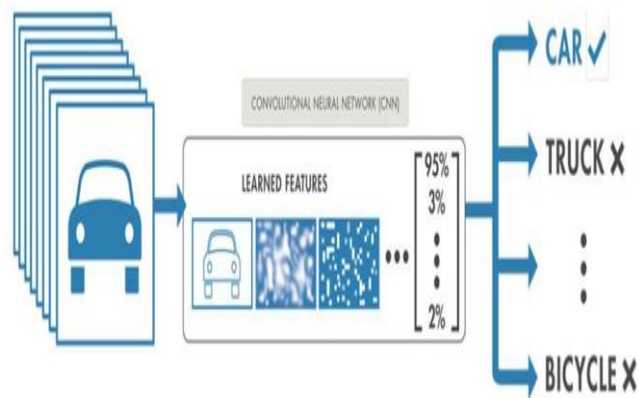


Fig. 2. Convolutional neural network that automatically learns features and classifies objects.

METHODOLOGY

The workflow for classifying brain MRI images is illustrated in Fig. 3. The proposed brain tumor detection method is structured into three main stages. Step 1: image processing (pre-processing, segmentation, contour detection of objects). Step 2: feature extraction using CNN (Resnet50). Step 3: detection based on the SVM classifier.

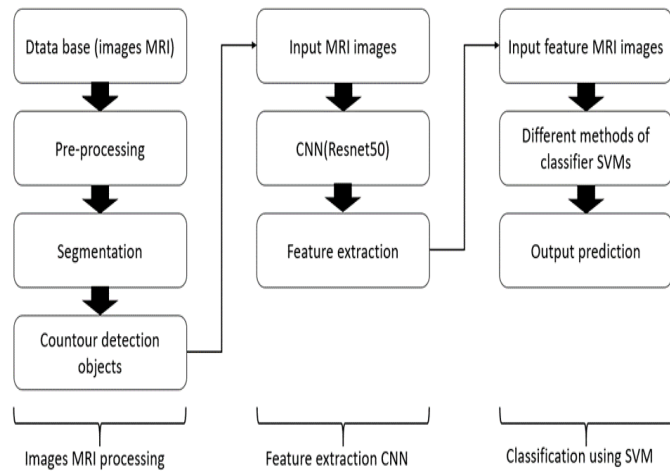


Fig. 3. MRI image feature selection diagram by Resnet 50 and classification based on the algorithm of different SVM methods.

Image processing

Database

Two sets of brain MRI images are used, 390 no tumor and 39 tumor in JPG image format, are extracted from the Kaggle database (Bhuvaji, 2020). Fig. 4.a shows healthy brain tumor images and Fig. 4.b brain images with tumor.

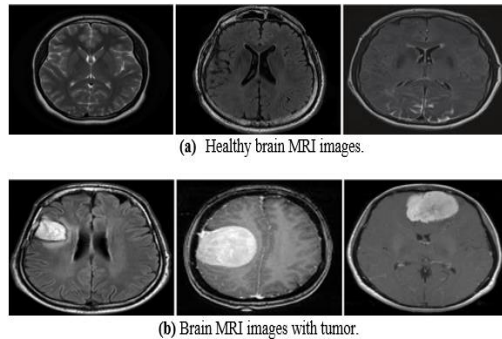


Fig. 4. Sample brain MRI images.

Pre-treatment

In this step, the method is used to improve the image quality and extract other useful information such as edge detection. These are mathematical morphology operations and pixel subtraction. First, MRI images are converted to grayscale, and padded to $3*3$ size to ensure the best filtering. Followed by a mathematical morphology based on dilation and erosion with a gamma four structuring element ($\Gamma 4$). Then pixel subtraction is applied for edging detection.

Mathematical morphology

Morphology is a large set of image-processing operations that are used to separate boundary objects and skeletons in an image (Maragos, 1996). Then, we can detect image contours with erosion and dilation (Hexmans, 1990). In this paper, the skeletal contours of the skull are extracted by applying dilation and erosion by the same gamma four structuring element. The subtraction of pixels is applied as a continuation; the dilated image is subtracted from the eroded image, which allows us to detect the contours as shown in Fig. 5.b.

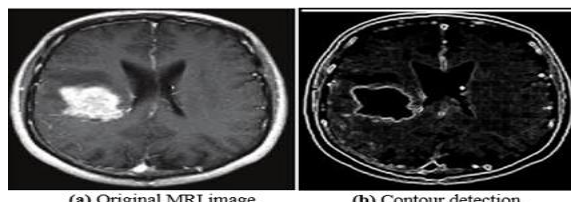


Fig. 5. Contour detection result by morphology.

Segmentation

Segmentation refers to the process of partitioning an image into multiple distinct regions based on visual attributes such as color intensity or geometric structure (Huang, 2014). Among various segmentation techniques, Otsu's method is commonly employed for determining an optimal threshold automatically by analyzing the distribution of pixel intensities in the image histogram, as illustrated in Fig. 6.

This method involves analyzing the histogram to determine a threshold that best separates the image into two pixel categories. It assumes that the image data is digital and can be modeled as belonging to two distinct classes. Through an iterative procedure, the algorithm determines the threshold value T that minimizes the variance within each class (intra-class variance), thereby maximizing class separation.

In our work, we apply the Otsu thresholding method to enhance brain MRI images after edge detection. The results of this process are shown in Fig. 7. The global threshold T is computed using MATLAB's built-in graythresh function, which identifies the value that minimizes the intra-class variance between foreground and background pixel intensities (Sha, 2016).

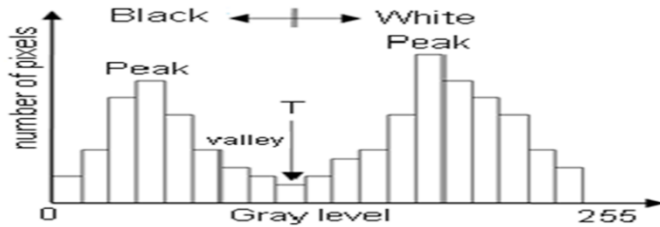


Fig. 6.Bimodal histogram with selected threshold "T".

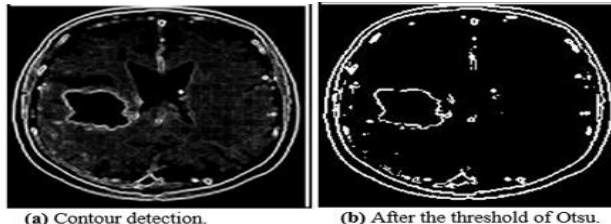


Fig. 7.Obtained results of the Otsu thresholding.

Object Contour Detection

Boundary tracing in binary images is a segmentation approach used to detect the edge pixels that delineate a digital region. It serves as a crucial initial step in the structural analysis of that region (Kovalevsky, 2021). After this step, we use the function "bwboundaries" with the option "noholes", to trace the outer boundaries of the objects, as well as the boundaries of the holes inside these objects, in the binary image (Narappanawar, 2010). Then our label images were converted to RGB color to visualize the labeled regions. The "label2rgb" function was used to determine the color to be assigned to each object according to the number of objects. The obtained results are presented in Fig. 8.

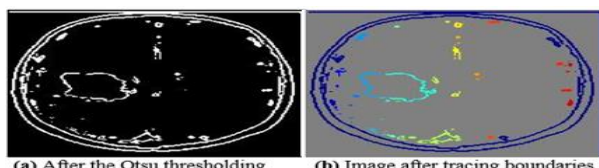


Fig. 8.Tracing the outer boundaries of MRI image objects.

Feature Extraction by ResNet50

Deep learning relies on the architecture of artificial neural networks (ANN), employing multiple hierarchical layers to automatically extract and transform features from input data. In our approach, the ResNet50 model is utilized during the feature extraction phase. This architecture, consisting of 177 layers, is a deep residual network with 50 convolutional layers and has been pre-trained on a dataset containing over one million images. It is capable of recognizing and categorizing input visuals into one of 1,000 distinct object classes (Krizhevsky, 2017; Simonyan, 2014).

Prepare Training and Test Image Sets

The training of our Residual Network is portioned in the following data, 70% of training containing 546 of healthy and tumor brain images, 30% of testing containing 234 of healthy and tumor brain images. Fig. 9 shows the division of our database which is taken randomly.

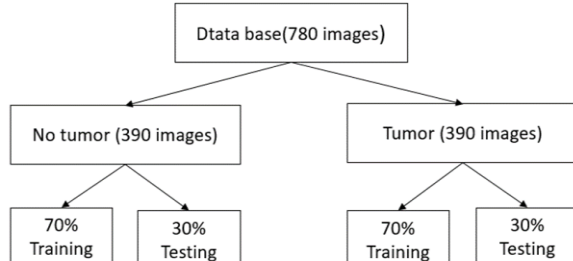


Fig. 9. Data base division.

Extract Training Features Using ResNet50

ResNet50 is a deep convolutional neural network consisting of 50 layers (Panda, 2022). Its architecture, illustrated in Fig. 10, begins with a convolutional layer that uses a kernel size of 7×7 with 64 filters and a stride of 2, forming the initial layer. This is followed by a max-pooling operation with a stride of 2. The next stage involves a sequence of convolutions with kernel sizes of 1×1 (64 filters), 3×3 (64 filters), and 1×1 (256 filters), repeated three times, contributing a total of 9 layers. The following block applies a similar pattern using 1×1 (128 filters), 3×3 (128 filters), and 1×1 (512 filters) kernels, repeated four times, resulting in 12 additional layers. This is followed by another sequence employing 1×1 (256 filters), 3×3 (256 filters), and 1×1 (1024 filters) convolutions, repeated six times to produce 18 more layers. Subsequently, a block with kernel sizes of 1×1 (512 filters), 3×3 (512 filters), and 1×1 (2048 filters) is repeated three times, adding 9 further layers. To conclude, the architecture incorporates an average pooling layer, which is followed by a fully connected layer with 1,000 output nodes. The final classification is performed using a Softmax activation function, which constitutes the last layer of the network. The complete structure is depicted in Fig. 10. The last obtained layer is named fully connected (fc1000), used to select features of our images. This will allow us to obtain a matrix of size (1000x546), where lines represent the number of features extracted for each image and columns represent the number of image drive (He, 2016; Ali, 2021).

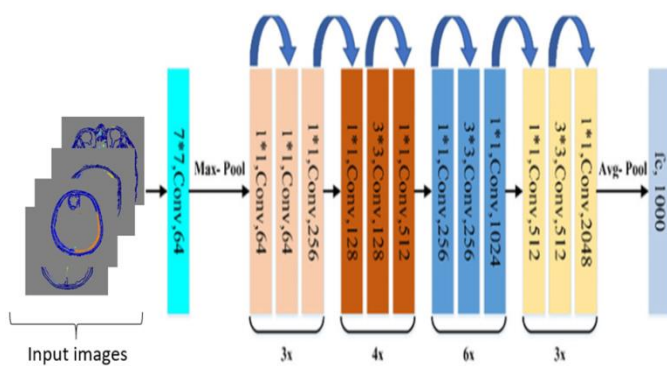


Fig. 10. Architecture of ResNet50 model.

Classification ResNet50

The ResNet50 architecture was tested with Test data containing 234 images. Where 117 images without tumors, 109 of them are correctly classified and 8 are misclassified. For 117 images with tumors, 100 are correctly classified and 8 are misclassified. The accuracy of the classification is 89% (Eq.1). These obtained results are shown in Table 1.

$$\text{Accuracy} = \frac{\text{TP} + \text{TN}}{\text{TP} + \text{TN} + \text{FN} + \text{FP}} \quad (1)$$

TP: True positive (The tumor is present and detected).

TN: True negative (Non-existent and undetected tumor).

➤ FP: False positive (The tumor does not exist and is detected).
 ➤ FN: False negative (The tumor exists and is not detected).

Table 1. Confusion matrix of ResNet50.

	No tumor	Tumor
No tumor	109 (TN)	8 (FP)
Tumor	17(FN)	100 (TP)

Classification using SVM-ResNet50 and Results

In this step several SVM learning algorithms have been used. What we aim is to learn the model from the input data set for classifying the brain tumor images. Four Kernel functions are used which are the Linear, Gaussian, Quadratic, and Cubic. The featured bag obtained by the layer "fc1000" Resnet50 in the form of a matrix size (546x1000) (rows represent the number of images and columns represent the number of features), is used for our learning algorithm, to train and test our MRI images, to obtain a better classification and prediction of the tumor. The feature bag separation is given as follows, 70% for training (382 images) and 30% for testing (164 images), labels are used for our data such as "0" image without tumor and "1" with tumor. Fig. 11 shows the obtained SVM classification.

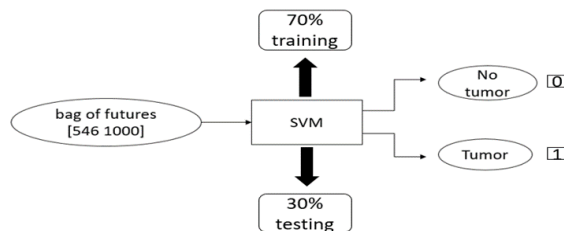


Fig. 11. Classification support vector machine.

Linear SVM

This represents the most basic scenario, in which the training data can be separated by a linear boundary (Roy, 2013). The corresponding linear function is defined in Eq 2.

$$f(x) = w^T x + b \quad (2)$$

For each training sample x_i , the function gives $f(x_i) \geq 0$, for $y_i = +1$ and $f(x_i) \leq 0$ for $y_i = -1$ (Singh, 2015).

The base data of two different classes are separated by the hyperplane $f(x) = w^T x + b = 0$ where w is the weight vector, b is the bias, x_i is the data. The characteristics of this model are shown in Table 2. The obtained results based on this model are given in Table 3.

Table 2. Linear SVM classifier features.

Classifier characteristics	
Preset	Linear SVM
Kernel function	Linear
Kernel scale	Automatic
Box constraint level	1
Multiclass method	One-vs-One
Standardize data	True

Table 3. Obtained results classifying linear SVM.

Accuracy	Prediction speed	Training time
92%	1200 obs/sec	6.2226 sec

From 81 images without tumors, we have 76 of them are correctly classified and 5 are misclassified. From 82 images with tumors, we have 74 of them are correctly classified and 8 are misclassified. The confusion matrix of the linear SVM model is presented in Fig. 12.

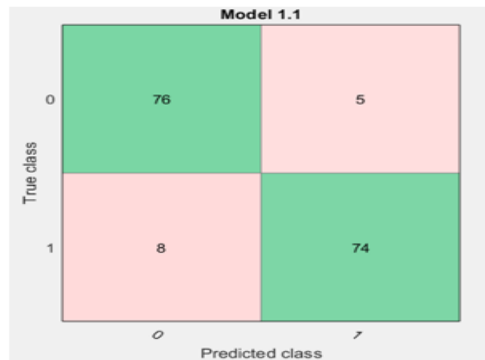


Fig. 12. Linear SVM model of the confusion Matrix.

Quadratic SVM

In this model we use the quadratic decision surface to separate the measurements of two or more classes of objects (Krishnakumar, 2021). The characteristics of this model are presented in Table 4. The quadratic function is given by Eq. 3.

$$f(x) = ax^2 + bx + c \quad (3)$$

The obtained results based on this method are presented in Table 5.

Table 5. Quadratic SVM classifier features.

Classifier characteristics	
Preset	Quadratic SVM
Kernel function	Quadratic
Kernel scale	Automatic
Box constraint level	1
Multiclass method	One-vs-One
Standardize data	True

Table 6. Obtained results classifying quadratic SVM.

Accuracy	Prediction speed	Training time
92%	1200 obs/sec	6.2532 sec

From 81 images without tumors, we have 75 of them are correctly classified and 6 are misclassified. From 82 images with tumors, 75 of them are correctly classified and 7 are misclassified. Figure 13 displays the confusion matrix associated with the quadratic SVM model.

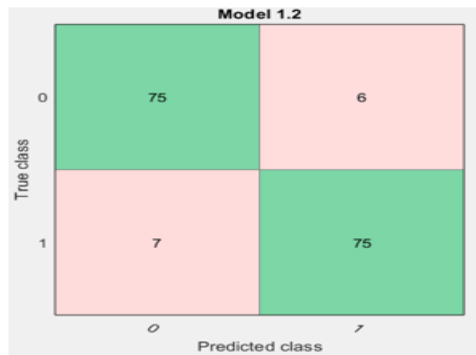


Fig. 13. Quadratic SVM model of the confusion Matrix.

Cubic SVM

The polynomial kernel is frequently applied in SVM models to measure the similarity between training vectors within a transformed feature space. By mapping the original variables into polynomial dimensions, it enables the learning of nonlinear decision boundaries (Amin, 2020). The characteristics of this model are shown in Table 6. The cubic polynomial Kernel function is given by Eq. 4.

$$k(x, y) = (x^T y + 1)^3$$

The obtained results using this method are presented in Table 7.

Table 7.Cubic SVM classifier features.

Classifier characteristics	
Preset	cubic SVM
Kernel function	Cubic
Kernel scale	Automatic
Box constraint level	1
Multiclass method	One-vs-One
Standardize data	True

Table 8.Obtained results classifying cubic SVM.

Accuracy	Prediction speed	Training time
93%	1300 obs/sec	7.1951 sec

From 81 images without tumors, we have 76 of them are correctly classified and 5 are misclassified. From 82 images with tumors, we have 76 of them are correctly classified and 6 are misclassified. Figure 14 presents the confusion matrix corresponding to the cubic SVM model.



Fig.14. Cubic SVM model of the confusion Matrix.

Medium Gaussian SVM

The medium Gaussian kernel is a widely used function in various machine learning algorithms, particularly in SVMs, as it effectively reduces both estimation and approximation errors in classification tasks (Ruan, 2007; Bahadure, 2017). The characteristics of this model are shown in Table 8. The Gaussian Kernel function is given by Eq. 5, where σ is the standard deviation.

$$k(x, y) = \exp\left(-\frac{\|x-y\|^2}{2\sigma^2}\right) \quad (5)$$

The obtained results using this method are presented in Table 9.

Table 9. Medium gaussianSVM classifier features.

Classifier characteristics	
Preset	Medium Gaussian SVM
Kernel function	Gaussian
Kernel scale	32
Box constraint level	1
Multiclass method	One-vs-One
Standardize data	True

Table 10. Obtained results classifying medium gaussianSVM.

Accuracy	Prediction speed	Training time
94%	1500 obs/sec	7.7308 sec

From 81 images without tumors, we have 77 of them are correctly classified and 4 are misclassified. From 82 images with tumors, we have 76 of them are correctly classified and 6 are misclassified. Figure 15 illustrates the confusion matrix corresponding to the cubic SVM classifier.



Fig. 15 Confusion matrix of the Medium Gaussian SVM model.

COMPARISON AND DISCUSSION

The different SVM methods used in this contribution are summarised in Table 10, where we present the obtained accuracy of each presented method and also with HarunBingol work (Bingol, 2021).

Table 11. Comparison obtained accuracy of each methods.

Present methods	Methods	Accuracy
	Resnet50	89%
	Linear SVM	92%
	Quadratic SVM	92%
	Cubic SVM	93%

 Harun BINGOL and al. (2021) (41)	Medium Gaussian SVM Deep Learning classification (Resnet50)	94% 85,71%
--	--	---------------

In this study, we adopted a hybrid methodology that integrates ResNet50 for feature extraction with multiple SVM classifiers to categorize brain tumor MRI images. The proposed approach yielded promising classification accuracies, ranging from 89% to 94%, depending on the specific SVM variant employed.

ResNet50 alone achieved an accuracy of 89% for tumor image identification, linear and quadratic SVMs reached an accuracy of 92%, cubic SVM achieved an accuracy of 93%, medium Gaussian SVM obtained the highest accuracy of 94%.

In comparison, the study by HarunBingol(Bingol, 2021), which also employs the ResNet50 architecture, reports an accuracy of 85.71% for brain tumor detection from MRI images. Bingol uses AlexNet, GoogLeNet, and ResNet50 architectures, with ResNet50 achieving the best accuracy among the three models.

The performance gap between our results and Bingol's can be attributed to several factors. Firstly, we used a similar dataset sourced from the Kaggle database, ensuring a relevant comparison. It is worth emphasizing that the preprocessing and segmentation techniques employed in our study differ from those used in Bingol's work. Specifically, our methodology involved a series of image enhancement steps, including contrast adjustment, Otsu thresholding, and morphological operations such as erosion followed by dilation to improve contour detection. These tailored preprocessing strategies likely contributed to the superior performance observed in our model.

Moreover, our hybrid approach combining ResNet50 for feature extraction with SVMs for classification appears to offer additional advantages over the standalone use of ResNet50. The SVM models, particularly the medium Gaussian SVM, demonstrated outstanding performance, surpassing Bingol's results in this classification task.

It is also worth noting that using a larger dataset or other regularization methods could further enhance our model's performance. In Bingol's work, although ResNet50 produced relatively good results, a more advanced combination with techniques such as SVMs could potentially push the accuracy beyond 85.71%.

CONCLUSION

In this contribution, we have presented a new approach to improve the accuracy to diagnose brain cancer. This approach to detect and identify the brain tumors is based on Otsu segmentation and classification using ResNet50. The obtained accuracy rate is 89%. The hybrid classification of different SVM and ResNet50, linear, quadratic, cubic, and medium Gaussian, their accuracy rate are: 92%, 92%, 93%, and 94% respectively. The Resnet50 architecture was applied for deep extraction of features from our MRI images. This is used for features in the SVM classification. For the Medium Gaussian SVM, we obtain the best accuracy rate (94%). In this part of results, we have observed that, the ResNet50 gives an important bag of features for the classification of our MRI images. On the other hand, the hybrid system between SVM and ResNet50 gives better accuracy than ResNet50 alone. But the Medium Gaussian SVM and the best hybridization with ResNet50 gave the highest accuracy rate of 94%.

REFERENCES

Abbood, A. A., Shallal, Q. M., & Fadhel, M. A. (2021). Automated brain tumor classification using various deep learning models: a comparative study. *Indonesian Journal of Electrical Engineering and Computer Science*, 21.

Ali, L., Alnajjar, F., Jassmi, H. A., Gocho, M., Khan, W., & Serhani, M. A. (2021). Performance evaluation of deep CNN-based crack detection and localization techniques for concrete structures. *Sensors*, 21, <https://doi.org/10.3390/s21062004>

Alqhtani, S. M., et al. (2024). Improved Brain Tumor Segmentation and Classification in Brain MRI With FCM-SVM: A Diagnostic Approach. *IEEE Access*, 12(January), 61312–61335. <https://doi.org/10.1109/ACCESS.2024.3342973>

Alsubai, S., Khan, H. U., Alqahtani, A., Sha, M., Sidra, A., & Mohammad, U. G. (2022). Ensemble deep learning for brain tumor detection. *Frontiers in Computational Neuroscience*. <https://doi.org/10.3389/fncom.2022.888334>

Amin, J., Sharif, M., Yasmin, M., & Fernandes, S. L. (2020). A distinctive approach in brain tumor detection and classification using MRI. *Pattern Recognition Letters*, 139, 118–127. <https://doi.org/10.1016/j.patrec.2020.09.002>

Anitha, V., & Murugavalli, S. (2016). Brain tumour classification using two-tier classifier with adaptive segmentation technique. *IET Computer Vision*, 10(1), 9–17. <https://doi.org/10.1049/iet-cvi.2015.0041>

Bahadure, N. B., Ray, A. K., & Thethi, H. P. (2017). Image analysis for MRI based brain tumor detection and feature extraction using biologically inspired BWT and SVM. *International Journal of Biomedical Imaging*, 2017. <https://doi.org/10.1155/2017/9749108>

Barnholtz-Sloan, J. S., Ostrom, Q. T., & Cote, D. (2018). Epidemiology of brain tumors. *Neurologic Clinics*, 36(3), 395–419. <https://doi.org/10.1016/j.ncl.2018.04.001>

Basthikodi, M., Chaithrashree, M., AhamedShafeeq, B. M., & Gurpur, A. P. (2024). Enhancing multiclass brain tumor diagnosis using SVM and innovative feature extraction techniques. *Scientific Reports*, 14(1), 26023. <https://doi.org/10.1038/s41598-024-60003-w>

Bingol, H., & Alatas, B. (2021). Classification of brain tumor images using deep learning methods. *Turkish Journal of Science and Technology*, 16(2), 332–344. <https://doi.org/10.33400/turkjsci.tech.805078>

Biswas, A., & Islam, M. S. (2023). A Hybrid Deep CNN-SVM Approach for Brain Tumor Classification. *Journal of Information Systems Engineering & Business Intelligence*, 9(1). <https://doi.org/10.20473/jisebi.v9i1.33767>

Blumenthal, D. T., Artzi, M., Liberman, G., Bokstein, F., Aizenstein, O., & Bashat, D. B. (2017). Classification of high-grade glioma into tumor and nontumor components using support vector machine. *American Journal of Neuroradiology*, 38(5), 879–884. <https://doi.org/10.3174/ajnr.A5125>

Chinnam, S., Sistla, V. P. K., & Kolli, V. K. K. (2019). SVM-PUK Kernel Based MRI-brain Tumor Identification Using Texture and Gabor Wavelets. *Traitement du Signal*, 36(5), 413–421. <https://doi.org/10.18280/ts.360502>

Cristianini, N., & Shawe-Taylor, J. (2000). *An Introduction to Support Vector Machines and Other Kernel-Based Learning Methods*. Cambridge University Press.

Fan, R. E., Chen, P. H., Lin, C. J., & Joachims, T. (2005). Working set selection using second order information for training support vector machines. *Journal of Machine Learning Research*, 6, 1889–1918.

Fernandez, M. C., & Guillevin, R. (2019). L'intelligence artificielle au service de l'imagerie et de la santé des femmes. *Imagerie de la Femme*, 29(3), 135–140. <https://doi.org/10.1016/j.femme.2019.06.001>

Gordillo, N., Montseny, E., & Sobrevilla, P. (2013). State of the art survey on MRI brain tumor segmentation. *Magnetic Resonance Imaging*, 31(8), 1426–1438. <https://doi.org/10.1016/j.mri.2013.05.002>

He, K., Zhang, X., Ren, S., & Sun, J. (2016). Deep residual learning for image recognition. In *Proceedings of the IEEE Conference on Computer Vision and Pattern Recognition* (pp. 770–778). <https://doi.org/10.1109/CVPR.2016.90>

Hexmans, H. J. A. M., & Ronse, C. (1990). The algebraic basis of mathematical morphology I. Dilations and erosions. *Computer Vision, Graphics, and Image Processing*, 50(3), 245–295. [https://doi.org/10.1016/0734-189X\(90\)90153-B](https://doi.org/10.1016/0734-189X(90)90153-B)

Huang, M., Yang, W., Wu, Y., Jiang, J., Chen, W., & Feng, Q. (2014). Brain tumor segmentation based on local independent projection-based classification. *IEEE Transactions on Biomedical Engineering*, 61(10), 2633–2645. <https://doi.org/10.1109/TBME.2014.2327030>

Kovalevsky, V. (2021). *Image Processing with Cellular Topology*. Springer Singapore Pte Ltd. <https://doi.org/10.1007/978-981-15-5947-8>

Krishnakumar, S., & Manivannan, K. (2021). Effective segmentation and classification of brain tumor using rough K means algorithm and multi kernel SVM in MR images. *Journal of Ambient Intelligence and Humanized Computing*, 12, 4739–4750. <https://doi.org/10.1007/s12652-020-01849-y>

Krizhevsky, A., Sutskever, I., & Hinton, G. E. (2017). Imagenet classification with deep convolutional neural networks. *Communications of the ACM*, 60(6), 84–90. <https://doi.org/10.1145/3065386>

Lesniak, M. S., & Brem, H. (2004). Targeted therapy for brain tumours. *Nature Reviews Drug Discovery*, 3(6), 499–508. <https://doi.org/10.1038/nrd1410>

Maragos, P. (1996). Differential morphology and image processing. *IEEE Transactions on Image Processing*, 5(6), 922–937. <https://doi.org/10.1109/83.503905>

Narappanawar, N. L., Rao, B. M., Srikanth, T., & Joshi, M. (2010). Vector algebra based tracing of external and internal boundary of an object in binary images. *Journal of Advanced Engineering Sciences*, 1(1), 1–7.

Noreen, N., Palaniappan, S., Qayyum, A., Ahmad, I., Imran, M., & Shoaib, M. (2020). A deep learning model based on concatenation approach for the diagnosis of brain tumor. *IEEE Access*, 8, 55135–55144. <https://doi.org/10.1109/ACCESS.2020.2981903>

Özkaraca, O., et al. (2023). Multiple Brain Tumor Classification with Dense CNN Architecture Using Brain MRI Images. *Life*, 13(2), 282. <https://doi.org/10.3390/life13020282>

Panda, M. K., Sharma, A., Bajpai, V., Subudhi, B. N., Thangaraj, V., & Jakhetiya, V. (2022). Encoder and decoder network with ResNet-50 and global average feature pooling for local change detection. *Computer Vision and Image Understanding*, 223, 103525. <https://doi.org/10.1016/j.cviu.2022.103525>

Ren, S., He, K., Girshick, R., & Sun, J. (2015). Faster R-CNN: Towards real-time object detection with region proposal networks. *Advances in Neural Information Processing Systems*, 28, 91–99.

Roy, S., Nag, S., Maitra, I. K., & Bandyopadhyay, S. K. (2013). A review on automated brain tumor detection and segmentation from MRI of brain. *arXiv preprint*. <https://arxiv.org/abs/1312.2240>

Ruan, S., Lebonvallet, S., Merabet, A., & Constans, J. M. (2007). Tumor segmentation from multispectral MRI images by using support vector machine classification. In *Proceedings of the 4th IEEE International Symposium on Biomedical Imaging* (pp. 496–499). <https://doi.org/10.1109/ISBI.2007.356974>

Ruppert, D. (2004). The Elements of Statistical Learning: Data Mining, Inference, and Prediction. *Journal of the American Statistical Association*, 99(466), 567–567. <https://doi.org/10.1198/jasa.2004.s339>

Saeedi, S., Rezayi, S., Keshavarz, H., & NiakanKalhori, S. R. (2023). MRI-based brain tumor detection using convolutional deep learning methods and chosen machine learning techniques. *BMC Medical Informatics and Decision Making*, 23(1), 1–17. <https://doi.org/10.1186/s12911-023-02152-7>

Sha, C., Hou, J., & Cui, H. (2016). A robust 2D Otsu's thresholding method in image segmentation. *Journal of Visual Communication and Image Representation*, 41, 339–351. <https://doi.org/10.1016/j.jvcir.2016.10.012>

Simonyan, K., & Zisserman, A. (2014). Very deep convolutional networks for large-scale image recognition. *arXiv preprint*. <https://arxiv.org/abs/1409.1556>

Singh, A. (2015). Detection of brain tumor in MRI images using combination of fuzzy c-means and SVM. In *Proceedings of the 2nd International Conference on Signal Processing and Integrated Networks* (pp. 98–102). IEEE. <https://doi.org/10.1109/SPIN.2015.7095308>

Sultan, H. H., Salem, N. M., & Al-Atabany, W. (2019). Multi-classification of brain tumor images using deep neural network. *IEEE Access*, 7, 69215–69225. <https://doi.org/10.1109/ACCESS.2019.2919122>

Suryawanshi, S., & Patil, S. B. (2024). Efficient Brain Tumor Classification with a Hybrid CNN-SVM Approach in MRI. *Journal of Advanced Information Technology*, 15(3), 340–354. <https://doi.org/10.12720/jait.15.3.340-354>

Zitnick, C. L., & Dollár, P. (2014). Edge boxes: Locating object proposals from edges. In *Computer Vision–ECCV 2014* (pp. 391–405). Springer. https://doi.org/10.1007/978-3-319-10602-1_26

Zhang, Z., Liu, P., Su, C., & Tong, S. (2025). A high-speed finger vein recognition network with multi-scale convolutional attention. *Applied Sciences*, 15(5), 1–15. <https://doi.org/10.3390/app15052698>